

# DEUTSCHES ELEKTRONEN – SYNCHROTRON

DESY 93-032  
March 1993



## First Order Electroweak Phase Transition

W. Buchmüller, Z. Fodor

*Deutsches Elektronen-Synchrotron DESY, Hamburg*

ISSN 0418-9833

NOTKESTRASSE 85 • D-2000 HAMBURG 52

DESY behält sich alle Rechte für den Fall der Schutzrechtserteilung und für die wirtschaftliche Verwertung der in diesem Bericht enthaltenen Informationen vor.

DESY reserves all rights for commercial use of information included in this report, especially in case of filing application for or grant of patents.

To be sure that your preprints are promptly included in the  
HIGH ENERGY PHYSICS INDEX,  
send them to (if possible by air mail):

**DESY  
Bibliothek  
Notkestraße 85  
W-2000 Hamburg 52  
Germany**

**DESY-IfH  
Bibliothek  
Platanenallee 6  
O-1615 Zeuthen  
Germany**

# First order electroweak phase transition \*

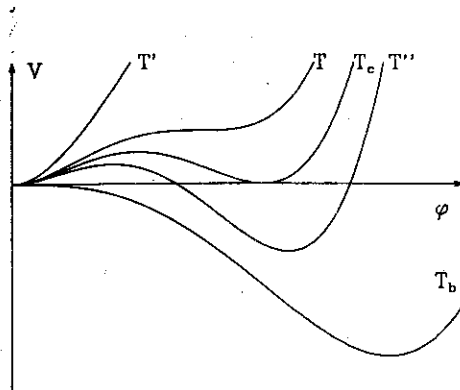
Wilfried Buchmüller and Zoltán Fodor<sup>1</sup>

*Deutsches Elektronen-Synchrotron DESY, Hamburg, Germany*

## 1. INTRODUCTION

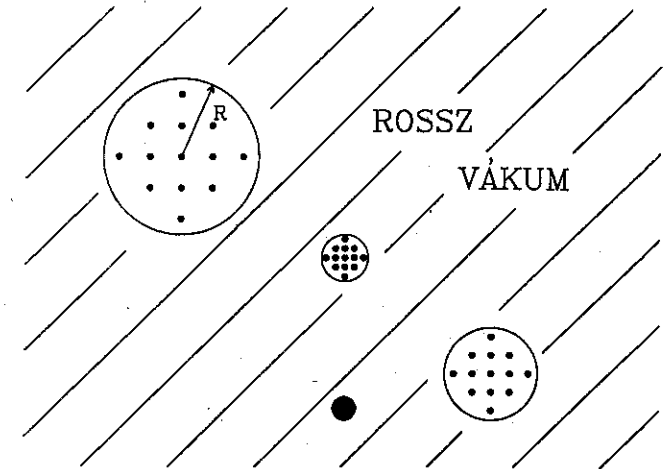
In the early universe at high temperatures the electroweak gauge symmetry has been restored<sup>2</sup>. This has important cosmological implications, since the baryon-number violating processes are unsuppressed<sup>3</sup> at high temperatures. In particular it is conceivable that the observed baryon asymmetry can be understood within the standard model (SM)<sup>4</sup>. In order to provide the necessary departure from thermal equilibrium a sufficiently strong first order phase transition via bubble nucleation is needed.

FIGURE 1. The effective potential at different temperatures



<sup>1</sup>Talk given at the Texas/PASCOS Symposium (December 1992, Berkeley, USA)

FIGURE 2. Bubble nucleation in the false vacuum



One basic ingredient in understanding this phenomenon is  $V_{eff}(\phi, T)$ , the temperature dependent effective potential, which is shown in fig. 1 as a function of the background field  $\phi$  for different temperatures  $T$ . At high temperatures the potential has only one global minimum at  $\phi = 0$ , the symmetry is restored. As the temperature decreases to  $T' < T$ , a second local minimum develops at  $\phi \neq 0$  which, at a critical temperature  $T_c$ , is degenerate with the minimum at  $\phi = 0$ . For temperatures  $T'' < T_c$  the local minimum at  $\phi = 0$  becomes metastable, and a barrier appears between the two minima. The corresponding phase transition is first order, since the change in the expectation value  $\phi$  is discontinuous. The physical picture at temperatures below  $T_c$  is the decay of the energetically unfavoured false vacuum. Thermal fluctuations cause bubbles of true vacuum (c.f. fig 2). If the bubble is too small, the gain in volume energy is smaller than the loss in surface energy, the bubble shrinks. However, for large enough bubbles it is energetically favourable to grow, converting the the false vacuum to true vacuum. At a given barrier temperature  $T_b < T''$  the minimum at the symmetric state disappears.

In order to understand this rather involved process, the electroweak phase transition, intensive theoretical work has been devoted to clarify details of  $V_{eff}(\phi, T)$  in the SM, e.g., to rule out the appearance of spurious linear terms and to solve related infrared problems. The kinetics of this phase transition has also attracted much attention. In the following we will analyse both questions. In sect. 2 we show the breakdown of the ordinary perturbative approach and use an improved one, where plasma masses are determined

from a set of one-loop gap equations. In our approximation  $g' = 0$ , thus the  $W$ -bosons and the  $Z$ -boson are degenerate in mass.  $V_{eff}(\varphi, T)$  is determined in next-to-leading order, i.e., including terms cubic in the gauge coupling  $g$ , the scalar self-coupling  $\lambda^{1/2}$  and the top-quark Yukawa coupling  $f_t$ . We analyse the influence of the higher order corrections on our results. By use of Langer's theory of metastability<sup>5</sup> we calculate in sect. 3 the nucleation rate of critical bubbles and determine the nucleation temperature of the cosmological phase transition. Sect. 4 contains our conclusions.

## 2. THE EFFECTIVE POTENTIAL

In the standard model the  $SU(2)$  doublet  $\Phi$  of scalar fields can be given as

$$\Phi = \frac{1}{\sqrt{2}} \begin{pmatrix} \chi_1 + i\chi_2 \\ \varphi + h + i\chi_3 \end{pmatrix}, \quad (1)$$

where  $h$  is the Higgs field,  $\chi_a$  ( $a = 1, 2, 3$ ) are the three Goldstone bosons and  $\varphi$  is a constant background field. In terms of the background field the tree-level potential is  $V_0(\varphi) = \mu\varphi^2/2 + \lambda\varphi^4/4$ . The temperature dependent one-loop corrections can be calculated using standard techniques<sup>6</sup>, here and in the following Landau gauge is chosen,

$$V_0(\varphi) + V_1^{(1)}(\varphi, T) = \frac{1}{2} \left( \frac{3g^2 + 8\lambda + 4f_t T^2 - \lambda v^2}{16} \right) \varphi^2 + \frac{1}{4} \lambda \varphi^4, \quad (2)$$

where the leading order high temperature expansion was used in the field dependent part. As is well known, this potential predicts a second order phase transition. The next order approximation in the high temperature expansion provides negative cubic terms in the tree-level vector boson mass  $m = g\varphi/2$ , the Higgs boson mass  $\tilde{m}_\varphi = \sqrt{\lambda(3\varphi^2 - v^2)}$  and the Goldstone boson mass  $\tilde{m}_\chi = \sqrt{\lambda(\varphi^2 - v^2)}$ . Note that  $\tilde{m}_\varphi^2$  and  $\tilde{m}_\chi^2$  are negative for small values of  $\varphi$ , thus the effective potential becomes complex. It can be shown that the loop expansion in any finite order can not cure this problem. Furthermore, the two-loop diagrams yield terms linear in  $m$ ,  $\tilde{m}_\varphi$  and  $\tilde{m}_\chi$ , and only an infinite summation of the ring diagrams gives the complete answer cubic in the couplings. There is another, more elegant way to perform the ring summation, namely the iterative solution of the gap equations. This method also enables us to estimate higher order corrections to our result. The basic idea behind this method is an improved perturbation theory, where loop diagrams are evaluated with boson propagators containing the exact masses  $m_{L,T}^2 = m^2 + \delta m_{L,T}^2$ ,  $m_{\varphi,\chi}^2 = \tilde{m}_{\varphi,\chi}^2 + \delta m_{\varphi,\chi}^2$ . The radiative corrections are treated as counter terms,

$$\delta S_\beta = -\frac{1}{2} \int_\beta dp \left[ \tilde{A}^\mu(p) (\delta m_L^2 P_{L\mu\nu} + \delta m_T^2 P_{T\mu\nu}) \tilde{A}^\mu(p) \right.$$

$$\left. - \delta m_\varphi^2 \tilde{\varphi}^2(p) - \delta m_\chi^2 \tilde{\chi}^2(p) \right], \quad (3)$$

and are determined self-consistently by solving gap equations at the corresponding loop order. In this approach the decomposition of the gauge-boson self-energy tensor

$$\Pi^{\mu\nu}(k) = \Pi_L^{\mu\nu}(k) P_L + \Pi_T^{\mu\nu}(k) P_T + \Pi_S^{\mu\nu}(k) S + \Pi_G^{\mu\nu}(k) P_G \quad (4)$$

yields the full propagator

$$\begin{aligned} \hat{D}(k) &= \sum_{n=0}^{\infty} D(k) [\Pi(k) D(k)]^n \\ &= \frac{-1}{k^2 - m^2 - \Pi_L(k)} P_L + \frac{-1}{k^2 - m^2 - \Pi_T(k)} P_T \end{aligned} \quad (5)$$

and the longitudinal and transverse plasma masses:

$$\delta m_L^2 = \Pi_L(0) = \text{Tr}[\Pi(0) P_L] = -\Pi_{00}(0), \quad (6)$$

$$\begin{aligned} \delta m_T^2 &= \Pi_T(0) = \frac{1}{2} \text{Tr}[\Pi(0) P_T] \\ &= -\frac{1}{2} [\Pi_\mu{}_\mu(0) + \Pi_L(0) + \Pi_G(0)], \end{aligned} \quad (7)$$

where the tensors  $\Pi_L^{\mu\nu}, \Pi_T^{\mu\nu}, \Pi_S^{\mu\nu}, \Pi_G^{\mu\nu}$  are functions of  $k^\mu$  and the rest frame four-vector  $(1, \vec{0})$ .

The relevant one-loop graphs for the gap equations are shown in fig. 3. Neglecting the logarithmic terms in the high temperature expansion one obtains the following set of equations to order  $g^3$  and  $\lambda^{3/2}$ :

$$m_L^2 = \frac{11}{6} g^2 T^2 + m^2 - \frac{g^2}{16\pi} \left( \frac{4m^2}{m_L + m_\varphi} + m_\varphi + 3m_\chi + 16m_T \right) T, \quad (8)$$

$$m_T^2 = \frac{g^2 T}{3\pi} m_T + m^2 - \frac{g^2}{6\pi} \left( \frac{m^2}{m_T + m_\varphi} - \frac{1}{8} \frac{(m_\varphi - m_\chi)^2}{m_\varphi + m_\chi} \right) T, \quad (9)$$

$$\begin{aligned} m_\varphi^2 &= \left( \frac{3g^2}{16} + \frac{\lambda}{2} + \frac{1}{4} f_t^2 \right) (T^2 - T_b^2) + 3\tilde{m}^2 \\ &\quad - \frac{3g^2}{16\pi} \left[ m_L + 2m_T + m^2 \left( \frac{1}{m_L} + \frac{2}{m_T} \right) \right] T \\ &\quad - \frac{3\lambda}{4\pi} \left[ m_\varphi + m_\chi + \tilde{m}^2 \left( \frac{3}{m_\varphi} + \frac{1}{m_\chi} \right) \right] T, \end{aligned} \quad (10)$$

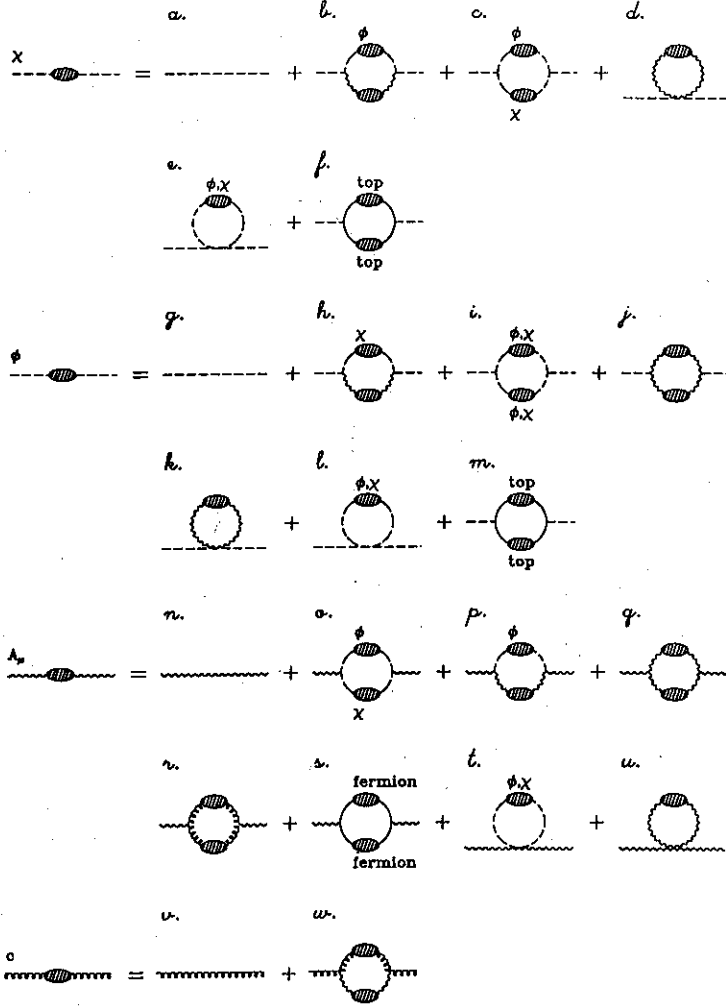
$$\begin{aligned} m_\chi^2 &= \left( \frac{3g^2}{16} + \frac{\lambda}{2} + \frac{1}{4} f_t^2 \right) (T^2 - T_b^2) + \tilde{m}^2 - \frac{3g^2}{16\pi} (m_L + 2m_T) T \\ &\quad - \frac{\lambda}{4\pi} \left( m_\varphi + 5m_\chi + \frac{4\tilde{m}^2}{m_\varphi + m_\chi} \right) T, \end{aligned} \quad (11)$$

where

$$m = g\varphi/2, \quad \bar{m} = \sqrt{\lambda}\varphi, \quad T_b^2 = \frac{16\lambda v^2}{3g^2 + 8\lambda + 4f_t^2}. \quad (12)$$

The ghost mass remains zero, and the mass corrections for fermions are not important since their Matsubara frequencies are always at least  $\mathcal{O}(1) \cdot T$ .

FIGURE 3. The SU(2) gap equations



The gap equations for the pure scalar theory ( $g = 0, f_t = 0$ ) at  $\varphi = 0$  and close to the barrier temperature gives  $m_\varphi \sim m_x \sim (T - T_b)$ , i.e.,  $m_\varphi$  and  $m_x$  approach zero with critical index one. This well-known result was first obtained by Dolan and Jackiw in the large- $N$  limit<sup>2</sup>. We obtain the same result, because at  $\varphi = 0$  only graphs *e*) and *l*) of fig. 3 contribute, which are the leading terms in the  $1/N$ -expansion.

The equation for the magnetic mass (9) is particularly interesting. At  $\varphi = 0$ , one has  $m_\varphi = m_x$ , and therefore  $m_T^2 = m_T g^2 T / (3\pi)$ . This equation<sup>7</sup> has two solutions,  $m_T = 0$ , and  $m_T = g^2 T / (3\pi)$ , but only the second solution is physical, since only  $m_T = g^2 T / (3\pi)$  can be continuously connected to a positive solution of eq. (9) at  $\varphi > 0$ .

The iterative solution of the gap equations with the lowest order mass corrections gives the effective potential

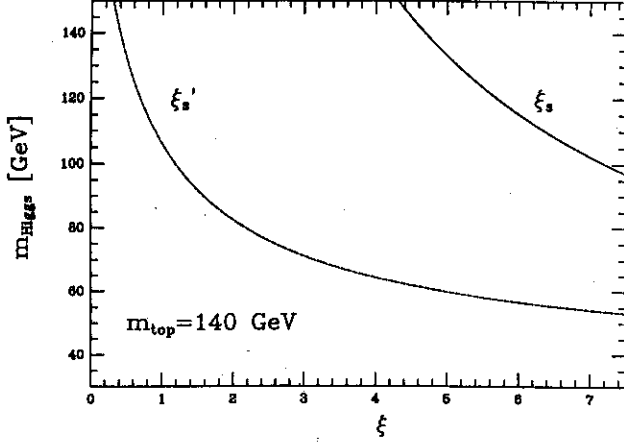
$$\begin{aligned} V_{gap}(\varphi, T) &= \int^\varphi d\varphi' \varphi' m_x^2(\varphi', T) = \frac{1}{2} \left( \frac{3g^2}{16} + \frac{\lambda}{2} + \frac{1}{4} f_t^2 \right) (T^2 - T_b^2) \varphi^2 \\ &+ \frac{\lambda}{4} \varphi^4 - \left( 3m_L^{(1)3} + 6m_T^{(1)3} + m_\varphi^{(1)3} + 3m_x^{(1)3} \right) \frac{T}{12\pi}, \\ m_L^{(1)2} &= \frac{11}{6} g^2 T^2 + m^2, \quad m_\varphi^{(1)2} = \left( \frac{3}{16} g^2 + \frac{\lambda}{2} + \frac{1}{4} f_t^2 \right) (T^2 - T_b^2) + 3\bar{m}^2, \\ m_T^{(1)2} &= m^2, \quad m_x^{(1)2} = \left( \frac{3}{16} g^2 + \frac{\lambda}{2} + \frac{1}{4} f_t^2 \right) (T^2 - T_b^2) + \bar{m}^2. \end{aligned} \quad (13)$$

Analyzing the infrared divergences in the gap equations one can estimate the convergence of this improved perturbative approach. If the condition

$$\xi \frac{\lambda T}{4\pi} \left( \frac{3}{m_\varphi} + \frac{1}{m_x} \right) \leq 1 \quad (14)$$

is satisfied one expects the uncertainty of the field-dependent part of the effective potential (13) to be of order  $1/\xi^2$ . According to fig. 1 the symmetric phase is metastable if for some  $\varphi > 0$  one has  $V(\varphi) \leq V(0)$ . Combining this conditions with eq. (14) one can determine the range of  $m_H$  and  $m_{top}$  where the phase transition is first order. The larger the Higgs mass, the more difficult it is to fulfill the  $\xi$ -condition (14). We have plotted in fig. 4 the maximal value of  $m_H$  for which this  $\xi$ -condition is just satisfied. The solid line is obtained by use of the masses with lowest order corrections, the dashed line corresponds to the  $\xi$ -condition with masses obtained from the gap equations. The more conservative dashed line suggest that the approximation is reliable if  $m_H < 80$  GeV, since in this case  $\xi' > 2$ . The result is rather insensitive to  $m_{top}$  in the mass range  $m_{top} = 100 - 200$  GeV.

FIGURE 4. The maximal allowed Higgs boson mass as a function of  $\xi$



### 3. BUBBLE NUCLEATION

In the metastable phase the probability distribution  $f(r)$  of small bubbles with radius  $r$  is given by the Boltzmann distribution  $f(r) \propto \exp(-\beta A_{\min}(r))$ , where

$$A_{\min}(r) = -\frac{8\pi\sigma}{3R}r^3 + 4\pi\sigma r^2 \quad (15)$$

is the work needed to form this bubble.  $R$  is the critical radius and  $\sigma$  is the surface tension. As already mentioned in the introduction small bubbles ( $r < R$ ) shrink, large bubbles ( $r > R$ ) grow. The Fokker-Planck equation gives the time dependence of the probability distribution, and a stationary solution yields the nucleation rate<sup>5</sup>

$$\Gamma = \frac{\kappa}{2\pi} \frac{\text{Im} Z_\beta[\bar{\Phi}]}{Z_\beta[\Phi=0]}, \quad (16)$$

where

$$\begin{aligned} Z_\beta[\bar{\Phi}] &= e^{-\beta F[\bar{\Phi}, T]} \\ &= \int_\beta [D\bar{\Phi}][DA_\mu][D\psi] e^{-\left(S_\beta[\bar{\Phi} + \hat{\Phi}, A_\mu, \psi] - \int_\beta dx \frac{\delta F[\bar{\Phi}, T]}{\delta \bar{\Phi}(x)} \hat{\Phi}(x)\right)}. \end{aligned} \quad (17)$$

The measure  $[DA_\mu]$  involves gauge fixing and ghost terms, and  $\psi$  stands for all fermion fields.  $\bar{\Phi}$  is a field configuration which interpolates between the symmetric and the broken phase. Since  $\bar{\Phi}$  is a stationary point of  $F$  we

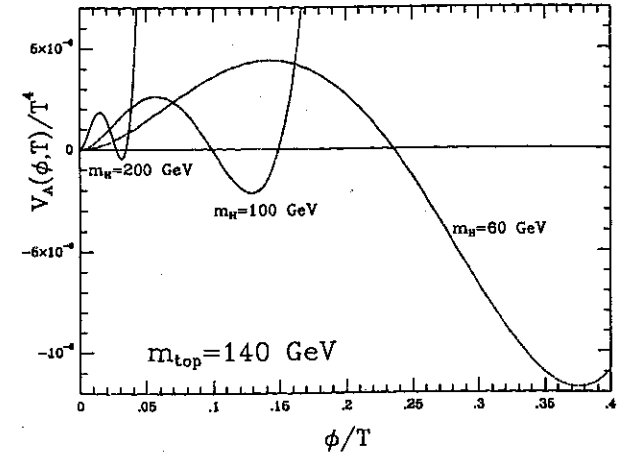
neglect the second term of the integrand in eq. (17). Evaluating the partition function in the saddle point approximation one obtains

$$\frac{\Gamma}{V} \approx \frac{\sqrt{2}}{2^9 \cdot 3^3 \cdot \pi^2 \lambda^3} g^9 \kappa (\beta\sigma)^{3/2} (\beta\mu)^{-3/2} (R\mu)^{41/8} e^{-\frac{4\pi}{3}\beta\sigma R^2}. \quad (18)$$

An important aspect of this approach is that scalar fluctuations are only computed around the stationary points  $\Phi = 0$  and  $\Phi = \bar{\Phi}$  and not, as usually done, around unstable homogeneous scalar background fields. Note, that the “dynamical factor”  $\kappa$  has been recently calculated.

Finally we discuss some features of the cosmological phase transition. A rough estimate of the temperature  $T_c$  at which the phase transition ends, is obtained by requiring  $\Gamma(t_c)t_c^4 \sim 1$ , where  $t \approx 0.03 \cdot m_{pl}/T^2$ . As an example we choose for the Higgs boson and top quark masses the values  $m_H = 70 \text{ GeV}$  and  $m_{top} = 140 \text{ GeV}$  respectively. Our previous discussion ensures that for these masses the higher order corrections are sufficiently small, and that the phase transition is first order. For this Higgs mass the longitudinal degree of freedom of the vector field decouples and the size of the cubic term in the effective potential is reduced by 1/3. For the temperatures  $T_c, T_e, T_b$ , the surface tension  $\sigma$ , the correlation length  $\xi$ , the width of the bubble wall  $d$  and the Higgs field  $\varphi_c$  at the second minimum we find  $T_c = 102 \text{ GeV}$ ,  $T_c - T_e = 0.02 \text{ GeV}$ ,  $T_c - T_b = 0.28 \text{ GeV}$ ,  $R = 2.9 \text{ GeV}^{-1}$ ,  $\sigma = 409 \text{ GeV}^3$ ,  $R/\xi = 10$ ,  $d/R = 0.25$ . We conclude that the thin wall approximation is marginally applicable and the phase transition is probably too weak to allow SM baryogenesis. We have plotted the potential for three different Higgs masses at the corresponding temperature  $T_c$  in fig. 5.

FIGURE 5. The potential for different Higgs boson masses at  $T_c$



#### 4. CONCLUSIONS

We have studied the phase transition in the  $SU(2)$  gauge theory at finite temperature. Our improved perturbative approach does not suffer from the infrared problems appearing in the ordinary loop expansion. We have calculated the effective potential up to cubic terms in the couplings. The higher order terms suggest that our method is reliable for Higgs masses smaller than  $80\text{ GeV}$ . We have obtained a non-vanishing magnetic mass which further weakens the transition.

By use of Langer's theory of metastability we have calculated the nucleation rate for critical bubbles and discussed some cosmological consequences. For  $m_H < 80\text{ GeV}$  the phase transition is first order and proceeds via bubble nucleation and growth. The thin wall approximation is only marginally applicable. Since the phase transition is quite weak SM baryogenesis is unlikely.

A detailed discussion of the results presented here and an extensive list of references can be found in ref. [8].

#### 5. NOTES AND REFERENCES

1. Humboldt Fellow, on leave from Institute for Theoretical Physics, Eötvös University, Budapest, Hungary.
2. D. A. Kirzhnits and A. D. Linde. 1972. Phys. Lett. B72: 471; S. Weinberg. 1974. Phys. Rev. D9: 3357; L. Dolan and R. Jackiw. 1974. Phys. Rev. D9: 3320.
3. V. A. Kuzmin, V. A. Rubakov and M. E. Shaposhnikov. 1985. Phys. Lett. B155: 36.
4. A.G. Cohen, D.B. Kaplan, A.E. Nelson. UCSD-PTH-93-02.
5. J. Langer. 1967. Ann. Phys. 41: 108; *ibid.* 1969. 54: 258.
6. J. I. Kapusta, Finite Temperature Field Theory, (Cambridge University Press, Cambridge, 1989).
7. This result has been independently obtained by J.R. Espinosa, M. Quirós and F. Zwirner, preprint CERN-TH.6577/92, IEM-FT-58/92.
8. W. Buchmüller, Z. Fodor, T. Helbig and D. Walliser, preprint DESY 93-021.